DIAGNOSTICS OF SOLAR IONS: Ne VI, Mg VI, Si VIII AND Mg VIII OBSERVED BY SERTS

B. N. DWIVEDI and ANITA MOHAN
Department of Applied Physics, Institute of Technology, Banaras Hindu University, Varanasi 221 005, India

(Received 9 April, 1994; in revised form 26 August, 1994)

Abstract. Diagnostics of solar ions Ne VI, Mg VI, Si VIII, and Mg VIII in an active region observed by SERTS have been presented. Density, temperature, and electron pressure in the emitting source have been derived from theoretical line-ratio curves and its EUV spectrum obtained by SERTS. The variation of neon-to-magnesium and silicon-to-magnesium abundances has been discussed in the interpretation of the active region spectrum obtained by SERTS.

1. Introduction

The inference of plasma temperature and density structure from spectral line ratios is a problem of universal importance for both laboratory and natural plasmas, in both of which fields there exists a vast literature including the recent review by Dwivedi (1994, and references therein). X-ray and EUV observations have clearly shown that the outer solar atmosphere is a complex region with no spherical symmetry, composed of coronal holes, characterised by open magnetic fields and by quiet and active regions with closed magnetic fields. The relevant region of the atmosphere, being anything but uniform and covering wide ranges in temperature and density poses a serious problem in the interpretation of observational data. Density-sensitive and temperature-sensitive line pairs give information on the average density and temperature structure independent of emitting volume. Ne VI and Mg VI have their respective maximum ionic concentrations at the same temperature, similarly for Si VIII and Mg VIII solar ions. The ionisation equilibrium curves for these ions overlap around temperatures of their respective maximum ionic concentrations as is shown in Figure 1 (Arnaud and Rothenflug, 1985).

Thomas and Neupert (1994) have presented wavelengths and absolute intensities averaged over one active region observed during the Solar EUV Rocket Telescope and Spectrograph (SERTS) flight of 5 May, 1989. A total of 243 emission lines were measured between 170–450 Å with a spectral resolution approaching 10 000. For this initial catalogue, the imaged spectra have been spatially averaged over a field of view 7 arc sec $\times$ 4.6 arc min, cutting through the centre of AR 5464 at S18 W45. The absolute intensities reported by Thomas and Neupert (1994) for Ne VI, Mg VI, Si VIII, and Mg VIII solar ions from NOAA Region 5464, a large, stable active region with a beta-gamma-delta magnetic configuration, whose largest sunspot was located at S18 W45 at the time of flight, form the basis of the

Solar Physics **156:** 81–94, 1995.

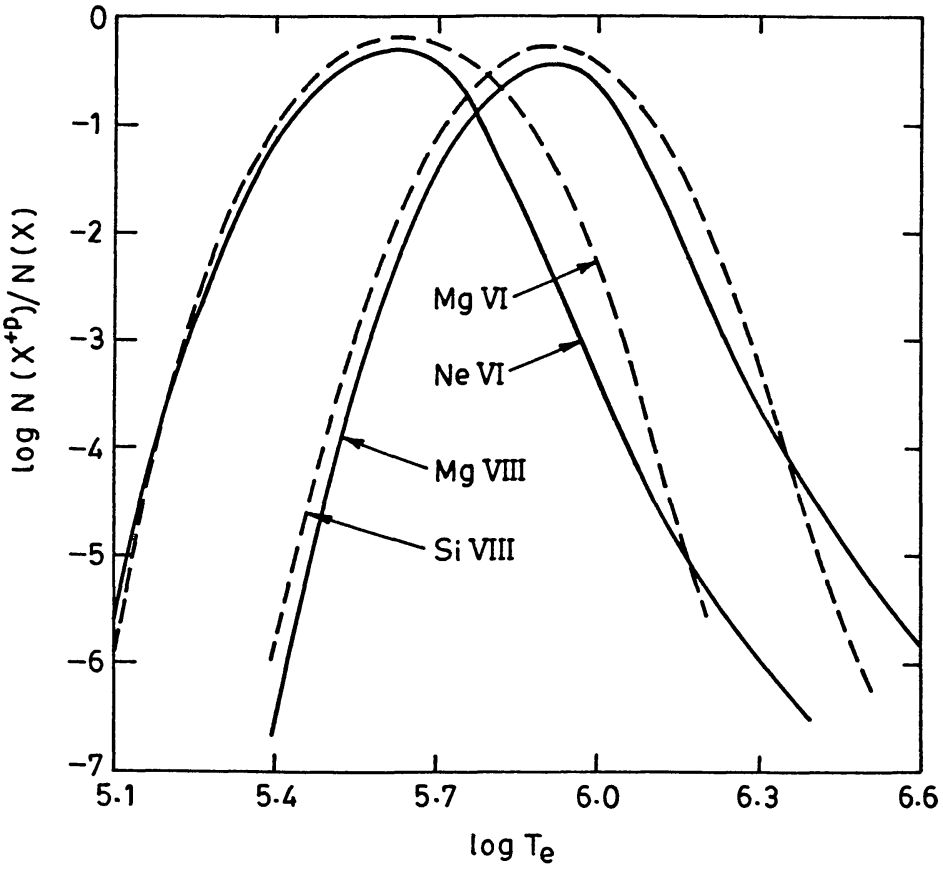

Fig. 1. Ionisation equilibrium curves for Ne VI, Mg VI and Si VIII, Mg VIII (from Arnaud and Rothenflug, 1985).

present investigation. We have computed several Ne VI/Mg VI and Si VIII/Mg VIII line emissivity ratios as a function of electron density and investigated density, temperature, and electron pressure in the active region from its EUV spectrum obtained by SERTS. The variation of neon-to-magnesium and silicon-to-magnesium abundances has also been discussed in the interpretation of the active region EUV spectrum obtained by SERTS.

In the following section, we briefly describe the line emissivities and the atomic data used in the present study. Observed and theoretical line intensity ratios are presented in the third section. Electron density and temperature diagnostics are examined in the fourth section. Concluding remarks are given in the last section.

2. Line Emissivity and Atomic Data

Taking account of atomic excitation mechanisms, the line emissivity per unit volume, per unit time, for an optically thin spectral line is given by the expression

$$\epsilon(\lambda_{ij}) = N_j A_{ji} \frac{hc}{\lambda_{ij}} (j > i) \,, \tag{1}$$

where A_{ji} is the spontaneous transition probability, h is Planck's constant, c is the velocity of light, and λ_{ij} is the wavelength for the transition $i-j$. N_j is the number density of level j. Thus the atomic physics problem reduces to the calculation of the population density of the upper excited level, j, which can be parameterised as

$$N_j(X^{+p}) = \frac{N_j(X^{+p})}{N(X^{+p})}\frac{N(X^{+p})}{N(X)}\frac{N(X)}{N(H)}\frac{N(H)}{N_e}N_e \,. \tag{2}$$

Here, X^{+p} is the pth ionisation stage of the element X; $N(X^{+p})/N(X)$ is the ionisation ratio of the ion X^{+p} relative to the total number density of the element (primarily a function of temperature for low electron densities); $N(X)/N(H)$ is the abundance of the element X relative to the hydrogen which may or may not be constant in the solar atmosphere; $N(H)/N_e$ is the hydrogen abundance which is usually assumed to be 0.8 for a fully ionised plasma; and finally $N_j(X^{+p})/N(X^{+p})$ is the population of level j relative to the total number density of the ion X^{+p} and is determined by solving the statistical equilibrium equations for the ion .

In the case of two lines emitted from the same ion, the line emissivity ratio can be expressed as

$$\frac{\epsilon(\lambda_{ij})}{\epsilon(\lambda_{kl})} = \frac{A_{ji}}{A_{lk}}\frac{\lambda_{kl}}{\lambda_{ij}}\frac{N_j(X^{+p})}{N_l(X^{+p})} \,. \tag{3}$$

The line emissivity ratio for the lines emitted from the same volume element but from different elements X and Y is then given by the expression

$$\frac{\epsilon(\lambda_{ij})}{\epsilon(\lambda_{kl})} = \frac{A_{ji}}{A_{lk}}\frac{\lambda_{kl}}{\lambda_{ij}} r(j,l,x,y)s(x,y)N(x,y) \,, \tag{4}$$

where

$$r(j,l,x,y) = \frac{N_j(X^{+p})}{N(X^{+p})} \Big/ \frac{N_l(Y^{+q})}{N(Y^{+q})} \,,$$

$$s(x,y) = \frac{N(X^{+p})}{N(X)} \Big/ \frac{N(Y^{+q})}{N(Y)} \,,$$

and

$$N(x,y) = \frac{N(X)}{N(H)} \Big/ \frac{N(Y)}{N(H)} \,.$$

In the above expressions, the line emissivity ratio depends on the relative ionic concentrations and abundances of the respective elements. As shown in Figure 1, the ionisation equilibrium curves (Arnaud and Rothenflug, 1985) for Ne VI and Mg VI ions overlap around the temperature of their maximum ionic concentration at 4×10^5 K; similarly for Si VIII and Mg VIII at 8×10^5 K. We therefore assume that lines from Ne VI and Mg VI ions originate from the same emitting layers; similarly for the ions Si VIII and Mg VIII. This assumption then justifies the use of Equation (4) for the line emissivity ratios. We have solved the steady-state equations for the various levels to obtain N_j(Ne VI)/N(Ne VI) and N_l(Mg VI)/N(Mg VI) as a function of electron density and temperature; similarly for Si VIII and Mg VIII ions. The first 11 lowermost energy levels for Ne VI and Mg VIII ions, and the first 13 energy levels are considered for Mg VI and Si VIII ions. The radiative transition probabilities and collision strengths for Ne VI and Mg VIII ions have been taken from Dankwort and Trefftz (1978) and Zhang, Graziani, and Pradhan (1994), respectively. These atomic data for Mg VI and Si VIII ions have been taken from Bhatia and Mason (1980).

3. Observed and Theoretical Line Ratios

Solar active region observation of EUV emission line intensities of Ne VI, Mg VI, Si VIII, and Mg VIII ions from SERTS are listed in Table I which forms the basis of the present study. Diagnostics of Ne VI and Mg VIII ions have been studied by several authors (Vernazza and Mason, 1978; Dwivedi and Raju, 1980; Dwivedi, 1988). Similarly, Mg VI and Si VIII ions have been studied (Feldman *et al.*, 1978; Dwivedi and Raju, 1988; Dwivedi, 1989, 1991). Recently, Raju and Gupta (1993) made an effort to explain the EUV line intensities of Ne VI and Mg VI ions corresponding to the average quiet-Sun conditions near solar minimum as observed by the ATM ultraviolet spectrometer on board *Skylab* (Vernazza and Reeves, 1978). They assumed a constant electron pressure ($N_eT_e = 6 \times 10^{14}$ cm^{-3} K) to estimate electron densities and temperatures within the chromosphere–corona transition region from Ne VI/Mg VI line ratios. While this assumption may be justified, we do not find any observed line-intensity ratios in their study for electron density measurement from theoretical line-ratio curves of Raju and Gupta (1993), probably because of the limiting spectral resolution of 1.6 Å of the ATM ultraviolet spectrometer. Moreover, theoretical line intensities computed by Raju and Gupta (1993), using a spherically symmetric solar atmospheric model of Elzner (1976), could only be very crudely used for estimating density and temperature from theoretical line-ratio curves under the assumption of constant electron pressure in the transition region. We believe that this kind of study could be quite misleading. We have, therefore, selected and studied line ratios from the two sets of ions, namely Ne VI and Mg VI, both of which have maximum ionic concentration around 4×10^5 K, and Si VIII and Mg VIII ions around 8×10^5 K. The solar active region EUV spectrum for these

TABLE I

SERTS observation of solar active region lines

Ion	Log T_e	Wavelength (Å)	Intensity (erg cm^{-2} s^{-1} sr^{-1})	Transition configuration	Terms
Ne VI	5.6	399.837	14.9	$2s^22p - 2s2p^2$	$^2P^0_{1/2} - ^2P_{3/2}$
		401.139	29.9	$2s^22p - 2s2p^2$	$^2P^0_{1/2} - ^2P_{1/2}$
		401.936	84.6	$2s^22p - 2s2p^2$	$^2P^0_{3/2} - ^2P_{3/2}$
		403.296[b]	46.1	$2s^22p - 2s2p^2$	$^2P^0_{3/2} - ^2P_{1/2}$
		433.161	7.5	$2s^22p - 2s2p^2$	$^2P^0_{1/2} - ^2S_{1/2}$
		435.632	9.8	$2s^22p - 2s2p^2$	$^2P^0_{3/2} - ^2S_{1/2}$
Mg VI	5.6	270.402	76.0	$2s^22p^3 - 2s2p^4$	$^2D^0_{5/2} - ^2P_{3/2}$
		349.162	55.2	$2s^22p^3 - 2s2p^4$	$^2D^0_{1/2,5/2} - ^2P_{3/2,5/2}$
		387.955	8.2	$2s^22p^3 - 2s2p^4$	$^2P^0_{3/2} - ^2D_{5/2}$
		399.275	9.3	$2s^22p^3 - 2s2p^4$	$^4S^0_{3/2} - ^4P_{1/2}$
		400.668	16.2	$2s^22p^3 - 2s2p^4$	$^4S^0_{3/2} - ^4P_{3/2}$
		403.296[b]	46.1	$2s^22p^3 - 2s2p^4$	$^4S^0_{3/2} - ^4P_{5/2}$
Si VIII	5.9	276.850	65.6	$2s^22p^3 - 2s2p^4$	$^2D^0_{3/2} - ^2D_{3/2}$
		277.045[b]	85.1	$2s^22p^3 - 2s2p^4$	$^2D^0_{5/2} - ^2D_{5/2}$
		314.345	54.1	$2s^22p^3 - 2s2p^4$	$^4S^0_{3/2} - ^4P_{1/2}$
		316.220	88.7	$2s^22p^3 - 2s2p^4$	$^4S^0_{3/2} - ^4P_{3/2}$
		319.839	113.0	$2s^22p^3 - 2s2p^4$	$^4S^0_{3/2} - ^4P_{5/2}$
Mg VIII	5.9	311.778[b]	79.1	$2s^22p - 2s2p^2$	$^2P^0_{1/2} - ^2P_{3/2}$
		313.735	80.6	$2s^22p - 2s2p^2$	$^2P^0_{1/2} - ^2P_{1/2}$
		315.024	253.0	$2s^22p - 2s2p^2$	$^2P^0_{3/2} - ^2P_{3/2}$
		317.008	57.5	$2s^22p - 2s2p^2$	$^2P^0_{3/2} - ^2P_{1/2}$
		339.000	53.8	$2s^22p - 2s2p^2$	$^2P^0_{3/2} - ^2S_{1/2}$
		430.445	40.3	$2s^22p - 2s2p^2$	$^2P^0_{1/2} - ^2D_{3/2}$
		436.727	68.1	$2s^22p - 2s2p^2$	$^2P^0_{3/2} - ^2D_{5/2}$

[b] indicates that the line is a blend.

ions from SERTS, having excellent spectral resolution of 0.005 Å, has been used to infer density, temperature and electron pressure in the emitting source.

In Figures 2(a)and 2(b) we have plotted the Ne VI to Mg VI line ratios as a function of electron density at $T_{max} = 4 \times 10^5$ K. Also plotted on the theoretical curves in Figures 2(a) and 2(b) are the line intensity ratios in the active region spectrum together with error limits in the value of the ratio. These line intensity ratios are dependent, in addition, on the relative element abundances and the relative ionic concentrations of Ne VI and Mg VI ions. Theoretical line ratio curves of Figures 2(a) and 2(b) are drawn for equal elemental abundances of Ne and

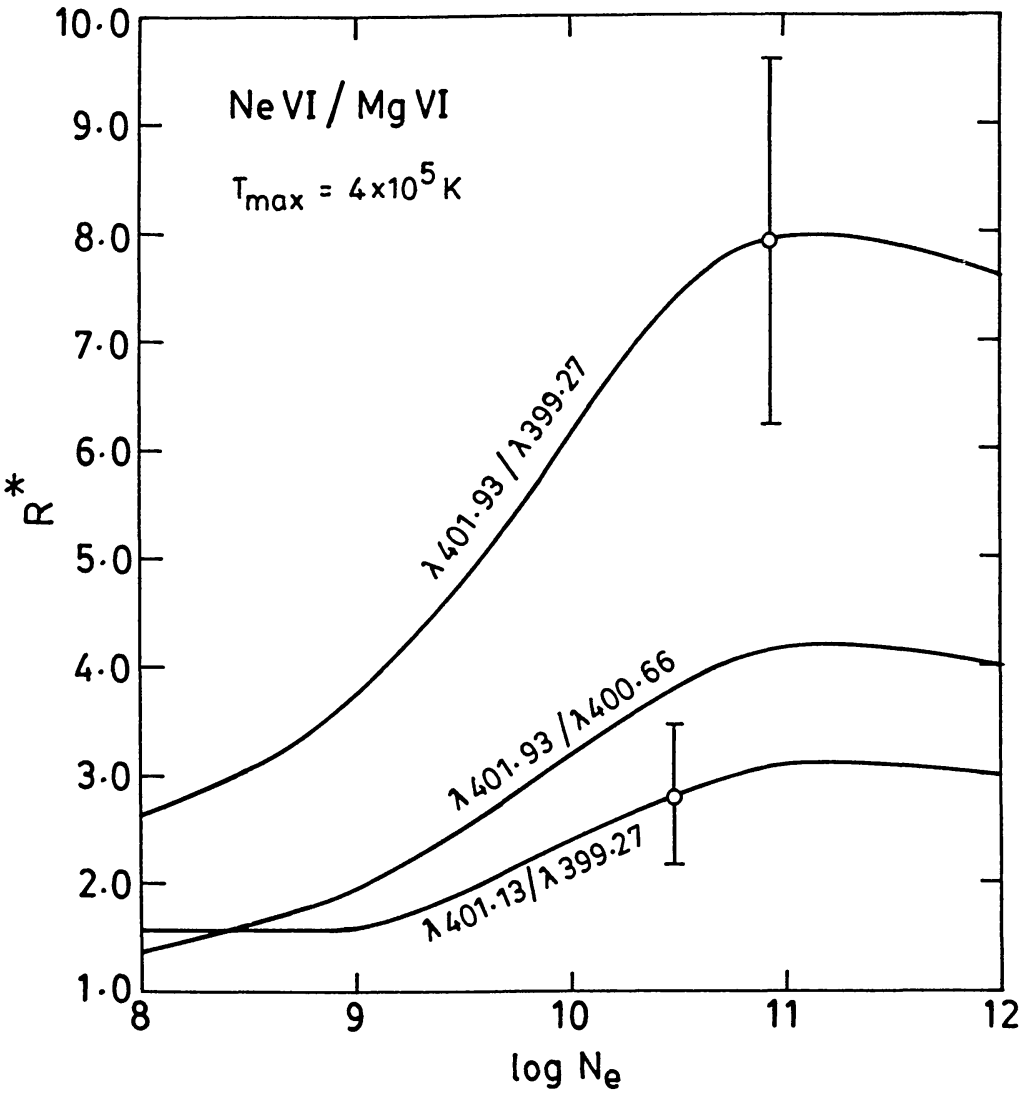

Fig. 2a.

Fig. 2a–b. Ne VI/Mg VI theoretical line-ratio curves at $T_{max} = 4 \times 10^5$ K as a function of electron density. The SERTS observed intensity ratios in the active region spectrum are shown by circles and error bars assuming Ne/Mg = 1.15.

Mg; that means these line ratio curves are the normalised values given by the expression

$$R^* = \left\{ \frac{\epsilon(\lambda(\text{Ne VI}))}{\epsilon(\lambda(\text{Mg VI}))} \right\}^{\text{normalized}} =$$

$$= \left\{ \frac{\epsilon(\lambda(\text{Ne VI}))}{\epsilon(\lambda(\text{Mg VI}))} \right\}^{\text{actual}} \Big/ \left\{ \frac{N(\text{Ne})}{N(\text{H})} \Big/ \frac{N(\text{Mg})}{N(\text{H})} \right\} . \quad (5)$$

Figure 3 shows the line ratios from Si VIII ion as a function of electron density at an electron pressure of 4×10^{16} cm^{-3} K. The circles and error bars in this figure refer to the line intensity ratios in the active region spectrum observed by SERTS. In

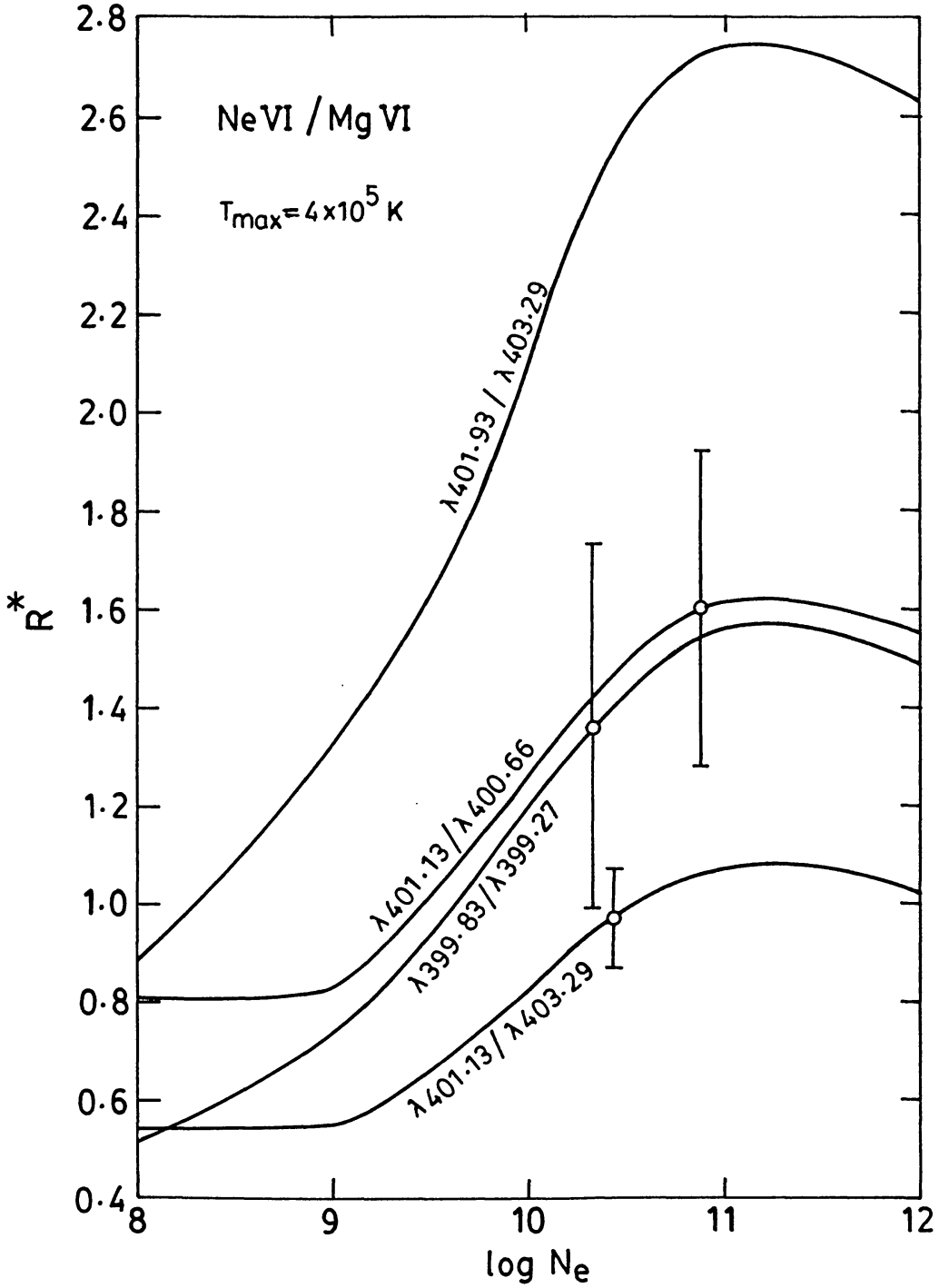

Fig. 2b.

Figures 4(a) and 4(b) we have plotted the Si VIII to Mg VIII line ratios as a function of electron density at $T_{max} = 8 \times 10^5$ K. These line-ratio curves are the normalised values in the same manner as discussed for Ne VI to Mg VI line ratios (cf., Equation (5)).

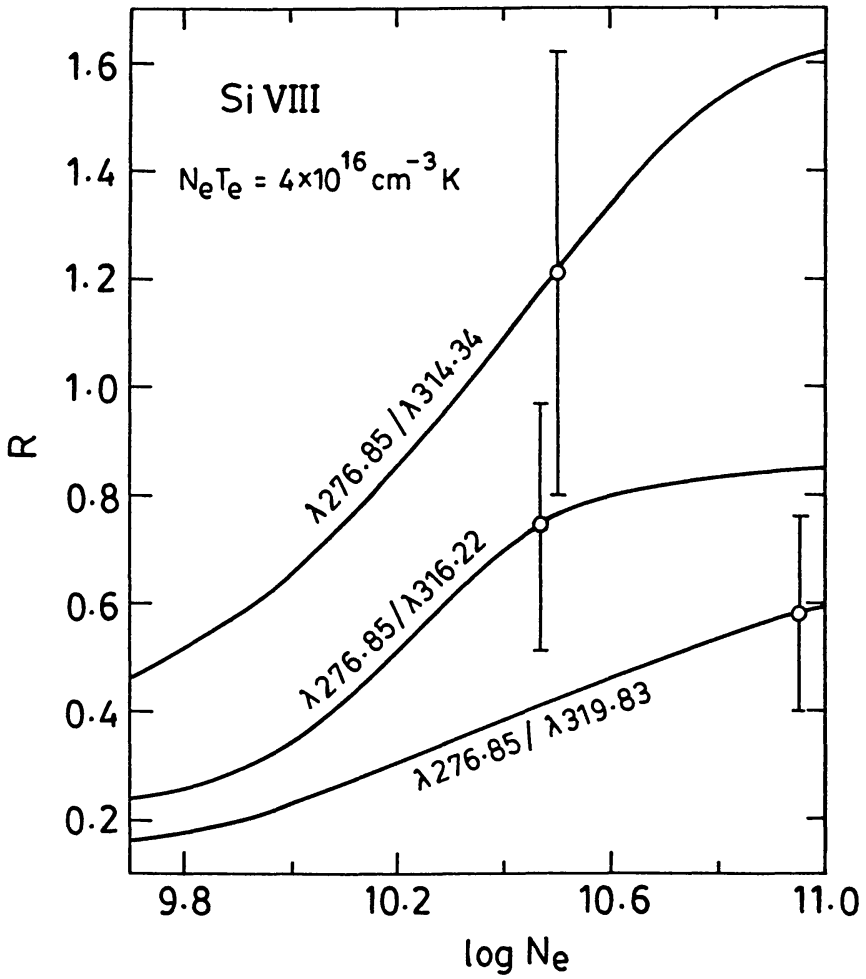

Fig. 3. Si VIII theoretical line-ratio curves for a constant value of electron pressure equal to $N_eT_e = 4 \times 10^{16}$ cm^{-3} K. The SERTS-observed intensity ratios in the active region spectrum are shown by circles and error bars.

4. Electron Density and Temperature Diagnostics

EUV lines from Ne VI and Mg VI ions predominantly carry the radiation signature of the solar transition region. The ionisation equilibrium curves for these ions essentially overlap each other (cf., Figure 1). In fact, various studies have shown that the quiet-Sun electron pressure within the chromosphere–corona transition region has almost a constant canonical value of 6×10^{14} cm^{-3} K (cf., Doschek, 1984). This cannot, however, explain the active region observation. The other two ions under investigation, Si VIII and Mg VIII, have their radiation signature of the upper transition region and the lower corona. The ionisation equilibrium curves for these ions also overlap each other (cf., Figure 1). It is, therefore, of much interest to investigate the density, temperature, and electron pressure in the active region using its excellent observation by SERTS.

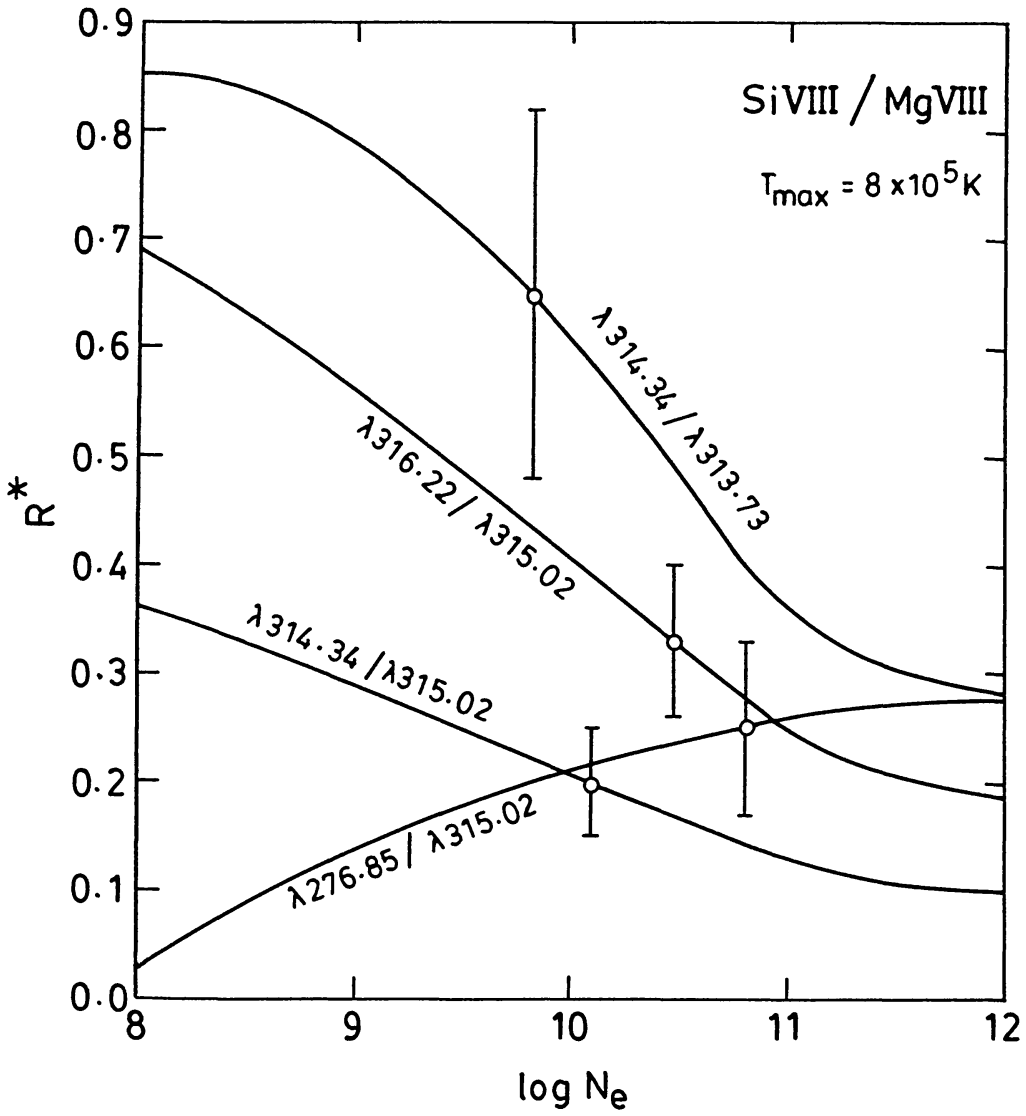

Fig. 4a.

Fig. 4a–b. Si VIII/Mg VIII theoretical line-ratio curves at $T_{max} = 8 \times 10^5$ K as a function of electron density. The SERTS-observed intensity ratios in the active region spectrum are shown by circles and error bars assuming Si/Mg = 1.05.

4.1. Diagnostics of Ne VI and Mg VI ions

The variation of the element abundance from the photosphere to the corona in different features of the solar atmosphere continues to be a topic of current research (Feldman and Widing, 1990; Feldman *et al.*, 1990; and Widing and Feldman, 1992). Such abundance variations will play a crucial role in the study of line diagnostics and our understanding of the coronal physical processes. The element abundances of Ne and Mg with respect to hydrogen are 3.5×10^{-5} and 3.7×10^{-5}, respectively (Meyer, 1985). Widing and Feldman (1989) have studied the neon-to-magnesium abundance variation in different features of the solar atmosphere and have found these variations to be strongly correlated with the magnetic field

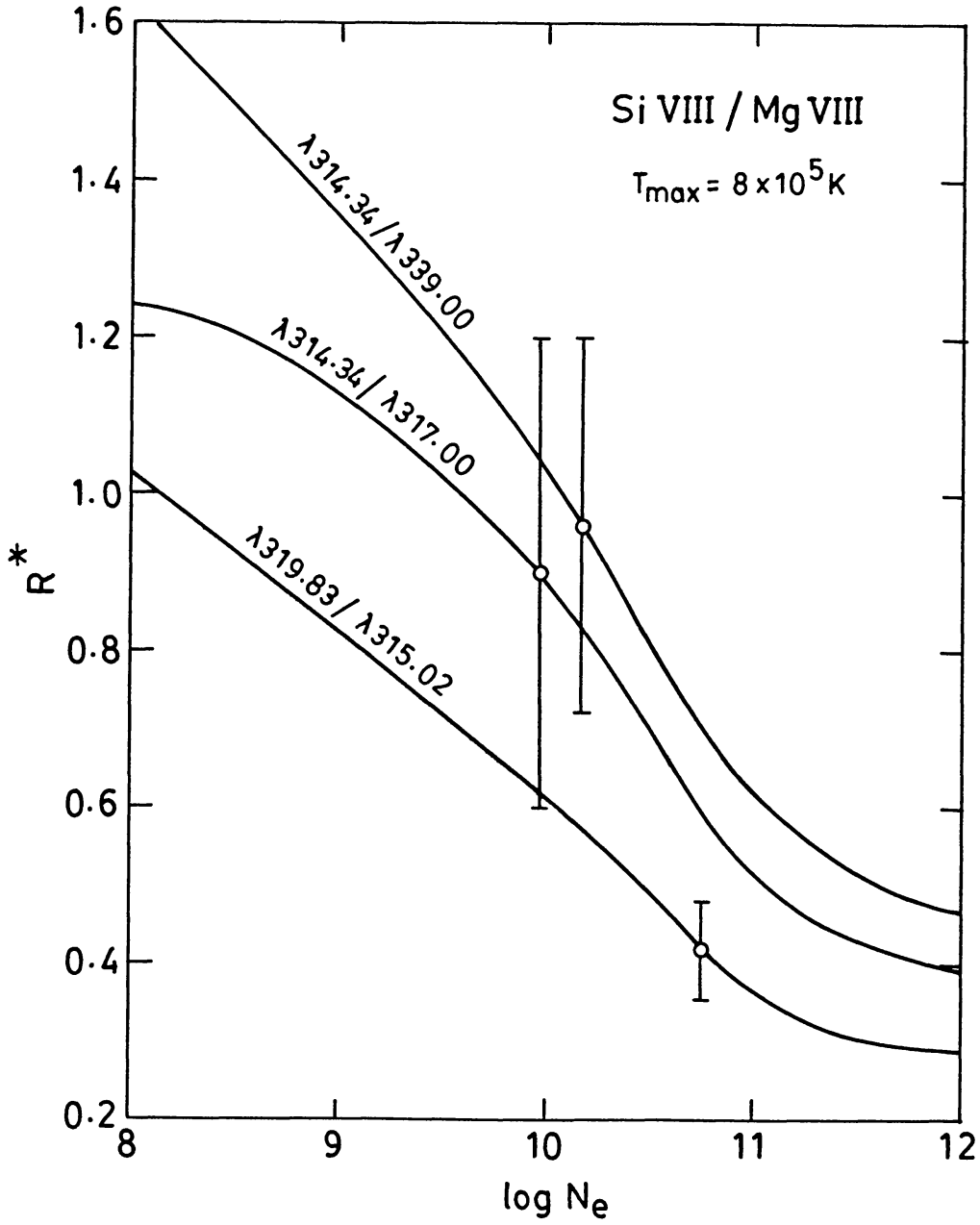

Fig. 4b.

morphology, ranging from Ne/Mg = 0.1 or 0.2 in some diffuse, open-field structures to values of 2 or 3 in some active, closed-field structures. These variations place a severe constraint on the inference of densities and/or temperatures from line-ratio diagnostics of two different ions. Widing and Feldman (1989) report a value of 0.64 in the active region for the Ne/Mg abundance ratio and its variation from 0.8 to 1.5 in active region loops and flare loops. We have, therefore, used an average of 0.8 and 1.5, that means Ne/Mg = 1.15, which may be a reasonable value for the active region (not completely representative of non-flaring active region) SERTS observation. Using Ne/Mg = 1.15 and absolute line intensities (cf., Table I), we

TABLE II

Electron densities inferred from Ne VI/Mg VI line ratios at $T_{max} = 4 \times 10^5$ K (cf., Figures 2(a) and 2(b))

Line pair (Å)	Normalised observed line-intensity ratio (R^*)	Inferred density N_e (cm^{-3})	N_eT_e (cm^{-3} K)
401.93/399.27	7.9	8.4×10^{10}	3.4×10^{16}
401.93/400.66	4.5	–	–
401.13/399.27	2.8	3×10^{10}	1.2×10^{16}
401.93/403.29[b]	2.8	–	–
401.13/400.66	1.6	7.5×10^{10}	3×10^{16}
399.83/399.27	1.4	2.1×10^{10}	8.4×10^{15}
401.13/403.29[b]	1	2.7×10^{10}	1.1×10^{16}

[b] indicates that the line is a blend.

have estimated electron densities from Ne VI/Mg VI theoretical line-ratio curves at $T_{max} = 4 \times 10^5$ K (cf., Figures 2(a) and 2(b)) and presented them in Table II. Circles and error bars in these figures represent the SERTS observations. It is to be noted that the Ne VI 403.29 and Mg VI 403.29 lines are blended. Using the atomic excitations for these two lines, we estimate that these Ne VI and Mg VI lines should have approximately intensities of 19.8 and 26.3 ergs cm^{-2} s^{-1} sr^{-1}, respectively, which have been used for density and/or temperature determinations. It is to be further noted that observed line intensities for Ne VI/Mg VI 401.93/403.29, 401.93/399.27, and 401.93/400.66 fall on the saturation region (about 10^{11} cm^{-3}) of the curves (cf., Figures 2(a) and 2(b)). Table II shows that electron pressure in the active region varies from 8.4×10^{15} to 3.4×10^{16} cm^{-3} K. In view of abundance anomalies, especially with regard to Ne VI/Mg VI, theoretical line ratios saturating beyond 10^{11} cm^{-3}, and above all error limits of about 30% in the theoretical curves and error limits on the observed line intensity ratios shown on the respective curves, no definite conclusion can be drawn. However, this result is indicative of density inhomogeneity in the active region under investigation.

4.2. Diagnostics of Si VIII and Mg VIII ions

An attempt has been made to interpret the SERTS observation of EUV emission lines from Si VIII and Mg VIII ions and to infer density and temperature structure in the active region. The celebrated density-sensitive Mg VIII λ430.44/λ436.72 line ratio, however, saturates at the active region densities and is not suitable for probing it. We find at least three density-sensitive Si VIII line ratios very well observed by SERTS, namely 276.85/314.34, 276.85/316.22, and 276.85/319.83, suitable for active region diagnostics. We have, therefore, studied these Si VIII line

TABLE III

Electron densities and temperatures inferred from Si VIII line ratios under a constant electron pressure $N_eT_e = 4 \times 10^{16}$ cm^{-3} K (cf., Figure 3)

Line pair (Å)	Observed line-intensity ratio (R)	N_e (cm^{-3}	T_e (K)
276.85/314.34	1.2	3.2×10^{10}	1.3×10^6
276.85/316.22	0.7	3×10^{10}	1.3×10^6
276.85/319.83	0.6	8.9×10^{10}	4.5×10^5

emissivity ratios as a function of density at the temperature of its maximum ionic concentration ($T_{max} = 8 \times 10^5$ K). The inferred densities have been found to be 3×10^{10}, 4.5×10^{10}, and 8×10^{10} cm^{-3}, respectively. These densities correspond to electron pressures of 2.4×10^{16}, 3.6×10^{16}, and 6.4×10^{16} cm^{-3} K, respectively, at $T_{max} = 8 \times 10^5$ K. It is, therefore, more appropriate to study these line ratios under an appropriate electron pressure in the emitting source. Accordingly, we have computed these line emissivity ratios at $N_eT_e = 4 \times 10^{16}$ cm^{-3} K (cf., Figure 3). Electron density and temperature values are restricted under the constant electron pressure. The densities derived from these theoretical line-ratio curves using the SERTS observation are given in Table III. Within the error limits of theoretical and observational values, we find that the density and temperature inferred are quite appropriate and consistent.

The solar abundance of Si relative to Mg for an active region is reported to be 1.05 (Widing and Feldman, 1989). Analysis by Widing and Feldman (1989) shows that the Si/Mg ratio is approximately constant in the EUV spectrum of the prominence and active region. This value of Si/Mg = 1.05 is, therefore, adopted to get the normalised line intensity ratios for the determination of active region densities from Si VIII/Mg VIII theoretical line-ratio curves at $T_{max} = 8 \times 10^5$ K (cf., Figures 4(a) and 4(b)) using the SERTS observation. The results obtained are listed in Table IV. This shows that electron pressure in the active region varies from 5.4×10^{15} to 5.0×10^{16} cm^{-3} K. In view of theoretical error limits of about 30% and observation error limits shown in respective figures, it is hard to make a definite estimate. However, one would tend to believe that electron pressure in the active region must vary to explain the observation. This conjecture is in good agreement with the results obtained by Nicolas *et al.* (1979) for active-region features.

TABLE IV

Electron densities inferred from Si VIII/Mg VIII line ratios at $T_{max} = 8 \times 10^5$ K (cf. Figures 4(a) and 4(b))

Line pair (Å)	Normalised observed line-intensity ratio (R^*)	Inferred density N_e (cm^{-3})	$N_e T_e$ (cm^{-3} K)
314.34/313.73	0.6	6.7×10^9	5.4×10^{15}
316.22/315.02	0.3	3.0×10^{10}	2.4×10^{16}
314.34/315.02	0.2	1.3×10^{10}	1.0×10^{16}
276.85/315.02	0.2	6.3×10^{10}	5.0×10^{16}
314.34/317.00	0.9	9.4×10^9	7.5×10^{15}
319.83/315.02	0.4	5.6×10^{10}	4.5×10^{16}
314.34/339.00	1	1.5×10^{10}	1.2×10^{16}

[b] indicates that the line is a blend.

5. Concluding Remarks

In conclusion, Ne VI/Mg VI and Si VIII/Mg VIII line emissivity ratios are found to be good candidates for active region diagnostics. This study is also in agreement with the density inhomogeneity in the solar atmosphere. A much more detailed analysis is underway taking account of many more suitable ions in the emitting source. Neon-to-magnesium and silicon-to-magnesium abundance ratios of 1.15 and 1.05, respectively, are found to satisfactorily explain the SERTS active region EUV spectrum. These EUV emission lines will be excellently observed by the Coronal Diagnostic Spectrometer (CDS) on board the Solar and Heliospheric Observatory (SOHO) scheduled for launch in 1995 by ESA/NASA.

Acknowledgements

We are indebted to Dr H. E. Mason for most helpful comments. Mrs Anita Mohan acknowledges financial support from the CSIR in the form of a Senior Research Fellowship.

References

Arnaud, M. and Rothenflug, R.: 1985, *Astron. Astrophys. Suppl.* **60**, 425.
Bhatia, A. K. and Mason, H. E.: 1980, *Monthly Notices Roy. Astron. Soc.* **190**, 925.
Dankwort, W. and Trefftz, E.: 1978, *Astron. Astrophys.* **65**, 93.

Doschek, G. A.: 1984, *Astrophys. J.* **279**, 446.
Dwivedi, B. N.: 1988, *Solar Phys.* **116**, 405.
Dwivedi, B. N.: 1989, *Solar Phys.* **123**, 385.
Dwivedi, B. N.: 1991, *Solar Phys.* **131**, 49.
Dwivedi, B. N.: 1994, *Space Sci. Rev.* **65**, 289.
Dwivedi, B. N. and Raju, P. K.: 1980, *Solar Phys.* **68**, 111.
Dwivedi, B. N. and Raju, P. K.: 1988, *Adv. Space Res.* **8**, No. 11, 179.
Elzner, L. R.: 1976, *Astron. Astrophys.* **47**, 9.
Feldman, U. and Widing, K. G.: 1990, *Astrophys. J.* **363**, 292.
Feldman, U., Widing, K. G., and Lund, P. A.: 1990, *Astrophys. J.* **364**, L21.
Feldman, U., Doschek, G. A., Mariska, J. T., Bhatia, A. K., and Mason, H. E.: 1978, *Astrophys. J.* **226**, 674.
Meyer, J. P.: 1985, *Astrophys. J. Suppl.* **57**, 151.
Nicolas, K. R., Bartoe, J. D. F., Brueckner, G. E., and Van Hoosier, M. E.: 1979, *Astrophys. J.* **233**, 741.
Raju, P. K. and Gupta, A. K.: 1993, *Solar Phys.* **145**, 241.
Thomas, R. J. and Neupert, W. M.: 1994, *Astrophys. J. Suppl.* **91**, 461.
Vernazza, J. E. and Mason, H. E.: 1978, *Astrophys. J.* **226**, 720.
Vernazza, J. E. and Reeves, E. M.: 1978, *Astrophys. J. Suppl.* **37**, 485.
Widing, K. G. and Feldman, U.: 1989, *Astrophys. J.* **344**, 1046.
Widing, K. G. and Feldman, U.: 1992, in E. Marsch and R. Schwenn (eds.), *Solar Wind Seven, COSPAR Colloquia Series*, Vol. 3, p. 405.
Zhang, H. L., Graziani, M., and Pradhan, A. K.: 1994, *Astron. Astrophys.* **283**, 319.